2023 IEEE International Symposium on Antennas and Propagation and USNC-URSI Radio Science Meeting (USNC-URSI) | 978-1-6654-4228-2/23/$31.00 ©2023 IEEE | DOI: 10.1109/USNC-URSI52151.2023.10237459

Wave-Controlled RIS: a Novel Method for Reconfigurable Elements Biasing

Miguel Saavedra-Melo, Kasra Rouhi, and Filippo Capolino
Department of Electrical Engineering and Computer Science, University of California, Irvine, CA 92617, USA

***Abstract*—A novel method for biasing the varactors of a reconfigurable intelligent surface (RIS) by using resonant standing waves on the biasing transmission line (TL) at a layer below the RF reflective surface to eliminate the need to bring external bias for each element of the RIS is described. We use an analytical model of the RIS to compare the field pattern of the reflected wave by (i) considering the ideal case, (ii) the case where reflection accounts for the varactor's model, and (iii) the case as in (ii) but where the biasing voltage distribution is constructed by using the wave control (i.e., standing waves).**

I. Introduction

Reconfigurable Intelligent Surfaces (RISs) are metasurfaces whose reflection properties can be changed by using an external signal to manipulate the reflected electromagnetic waves. It is usually designed with varactors that act as voltage-controllable capacitors. As a result, different voltage biases are applied to varactors in adjacent unit cells, and the ”locally reflected field” undergoes a controllable phase shift. RIss provide an excellent way to maximize the spectrum and energy efficiency of wireless communication systems at a low cost [1]; however, controlling the reconfigurable elements still remains a challenge, like the intense wiring of the RIS (one or two, at least per unit cell or small block of cells). The method proposed in [2] and here further analyzed faces such challenge and can be applied to any possible RIS unit cell geometry.

II. Description of the Method

This method consists of extracting the biasing voltage from the so-called ”biasing transmission line (TL)” [2]. The biasing TL supports resonant standing waves along the dimensions of the RIS. Then, each varactor can be connected to a specific location in the biasing TL, after the detector, to be biased according to the specific location-dependent voltage. In order to demonstrate the concept, a linear array of reconfigurable elements is analyzed. The normalized scattered pattern in the far-field region of a RIS made of N elements with separation d is

$$F(\theta) = \frac{1}{N}\sum_{n=1}^{N} R_n e^{j(n-1)kd\sin(\theta)+j\alpha_n}, \tag{1}$$

where R_n is the magnitude of the local reflection coefficient of the nth element, $k = 2\pi/\lambda$ is the wavenumber, and α_n is the reflected phase associated with that element. Assuming normal incidence, ideally $\alpha_{n+1}-\alpha_n = -\frac{2\pi}{\lambda} d\sin(\theta_{max})$ that produces a reflection along $\theta_{max.}$, the direction of maximum radiation (it can be generalized to multiple beams). In order to provide an estimate of RIS reflection properties when controlled by varactors, we use the analytical model presented in [3]. This model includes the data sheet information of the varactor with different DC biasing to obtain the values of R_n and α_n.

To bias the varactors, a TL of length $L = (N-1)d$ along the x direction is used (see geometry in [2]), which does not interfere with the incident and reflected RF waves while supporting modes that travel with phase velocity $v_b = c/n_{eff}$, where n_{eff} is the effective refractive index of the microstrip biasing TL. The number of biasing modes in the TL, P, is the number of degrees of freedom to control the response of the RIS. The fundamental biasing mode has a propagation wavenumber $k_{b,1}$ and a guided wavelength $\lambda_{b,1} = 2\pi/k_{b,1}$. In a realistic scenario, the biasing TL may be chosen to be electrically longer (L_t instead of L) than the size of the RIS by a small extra electric length $L_e = N_e d$ on each side to better control the voltages at the two ends of the standing waves. The fundamental standing wave on the biasing TL is excited by injecting proper frequencies into the TL such that $\lambda_{b,0} = 2L_t$. Therefore, the bias signal frequency is $f_{b,1} = (\lambda/(2n_{eff}L_t))\, f$. This frequency is generally smaller than the frequency f of the RF wave. Higher order standing waves have $f_{b,p} = pf_{b,1}$, with $p = 1, 2, ...$ The sum of the standing waves provides the polarization bias to a varactor at positions $x = (n-1)d$. The voltage representation of the sum of P standing waves is

$$v_P(x) = V_0 + \sum_{p=1}^{P} V_p \sin\left(\frac{p\pi}{L_t}x + \phi_{e,p}\right), \tag{2}$$

which consists of the summation of a DC bias V_0 and P standing waves with an amplitude of V_p. The wavenumber for the pth standing wave is $k_{b,p} = pk_{b,1}$. By properly choosing the excitation of each biasing TL mode, we can provide a large degree of variation in the varactor biasing. The standing waves are excited by using *a single port* where a time-domain periodic signal with a prescribed waveform is injected into the biasing TL, with a fundamental frequency $f_{b,1}$. The shape of the time-periodic voltage signal determines the coefficients V_p, and the amplitude of each term by assuming zero phase shift, i.e., $\phi_{e,p} = 0$, is given by

$$V_p = \frac{2}{L_t}\int_0^{L_t} (v(x) - V_0)\sin\left(\frac{p\pi}{L_t}x\right) dx. \tag{3}$$

III. Results and Discusion

The RIS used here as an example to evaluate the proposed method is based on [3]. The unit cell is a square patch backed by a grounded dielectric substrate and its geometry is shown in Fig. 1(a). It uses a grounded substrate RT5880LZ, with relative permittivity $\epsilon_r = 2$ and tan $\delta = 0.0021$. Adjacent

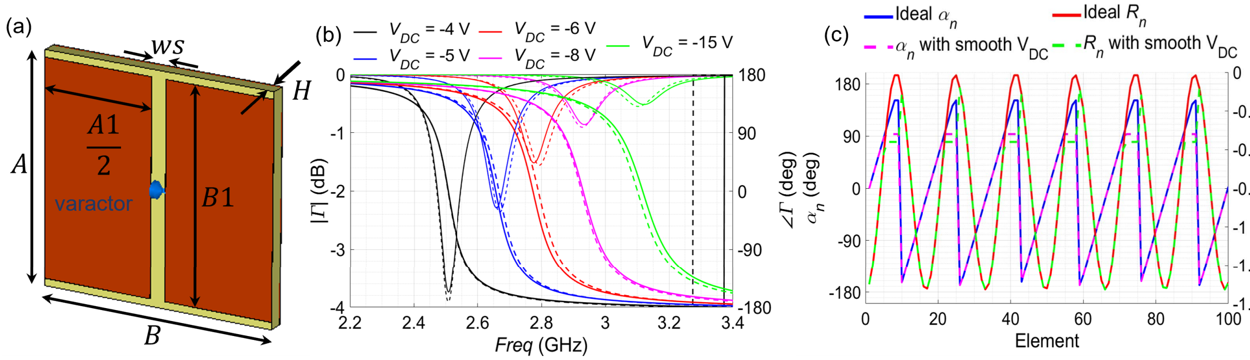

Fig. 1. (a) Unit cell with a varactor. In mm: $A = B = 19$, $A1 = B1 = 17.8$, $H = 1.27$, and $ws = 1.2$. (b) Magnitude and phase of the RIS reflection coefficient for different biasing voltages. The agreement between the analytical model (solid) and a full-wave simulation (dashed) is shown. (c) Magnitude and phase of reflection coefficients over the array of 100 elements, assuming $\theta_{max} = -20°$; the case for a smoothed out voltage distribution is also shown.

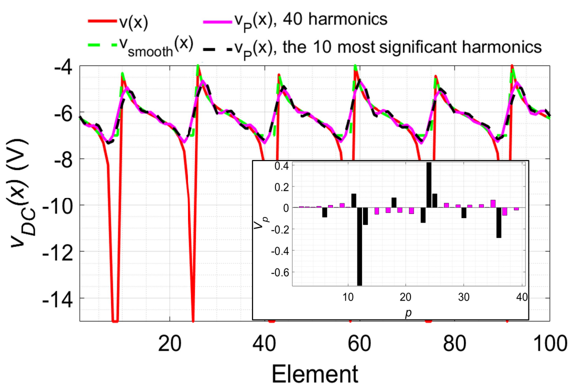

Fig. 2. Voltage distribution over a linear array of 100 elements to obtain a reflected beam pointing to $\theta_{max} = -20°$. The smoothed biasing voltage distribution (dashed green) avoids high voltage variations between adjacent elements while still redirecting the beam in the desired direction. The reconstructed biasing voltage distributions (2) in magenta and dashed black are obtained by using harmonics (3) with amplitudes shown in the inset.

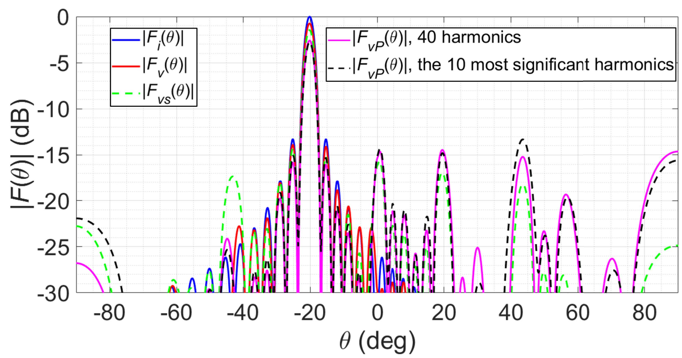

Fig. 3. Reflection scattering pattern of an array made of 100 elements, upon normal incidence and pointing to $\theta_{max} = -20°$. Patterns: F_i is the ideal one with linear phasing and no attentuation, F_v considers the effect of the varactors (losses and parasitics), F_{vs} considers the effect of the varactors with a smoothed out voltage distribution (Fig. 2), the two F_{vP} are obtained by using the biasing voltage standing waves as in (2).

patches are separated by a gap with a varactor diode. The chosen varactor is SMV1231-040LF, given its low series inductance of 0.45 nH and resistance of less than 0.5 Ω. The capacitance tuning range is limited to 0.46 - 0.8 pF. The commercial software CST Studio Suite is used to obtain the reflection coefficient by including the effect of the varactor as a lumped load in a periodic boundary condition. Assuming normal incidence, the amplitude and phase of the reflection coefficient of the reconfigurable unit cell for various varactor reverse bias voltages are plotted in Fig. 1(b), using both the analytical model from [3] and the full-wave simulation, in good agreement, where the phase tuning range is at least 260° and it is maintained across the band 2.55 - 3.05 GHz (500 MHz).

As an example, a linear array of 100 elements is considered. In Fig. 1(c) the distribution of the phase and magnitude of the reflection coefficient along the linear array is presented. In order to avoid sharp voltage variations along the RIS (to limit the overall number of degrees of freedom, i.e., the number P of standing waves), we smooth out the voltage distribution. In Fig. 2, the biasing voltage distribution across the RIS to obtain a reflected beam pointing to $\theta_{max} = -20°$ is shown. Also, a smoothed out biasing voltage distribution (dashed green) is included in this plot. The reconstructed voltages via (2) are also shown (magenta and dashed black) where it can be seen that only a few standing waves are required to construct the signal (in this example the 10 most significant harmonics are used).

Finally, in Fig. 3, the generated reflection scattering pattern pointing to $\theta_{max} = -20°$ is presented. We also show that the case with a smoothed-out voltage distribution leads to a similar reflection pattern, as well as the two cases with a bias distribution constructed with standing waves. The smoothness of the voltage distribution has not a significant impact on the general reflection performance of the RIS, hence a reduced number of degrees of freedom can be used.

ACKNOWLEDGEMENT

This material is based upon work supported by the USA National Science Foundation Award 2030029. The authors thank DS SIMULIA for providing CST Studio Suite.

REFERENCES

[1] S. Abeywickrama, R. Zhang, Q. Wu, and C. Yuen, "Intelligent reflecting surface: Practical phase shift model and beamforming optimization," *IEEE Transactions on Communications*, vol. 68, no. 9, pp. 5849–5863, 2020.

[2] E. Ayanoglu, F. Capolino, and A. L. Swindlehurst, "Wave-controlled metasurface-based reconfigurable intelligent surfaces," *IEEE Wireless Communications*, vol. 29, no. 4, pp. 86–92, 2022.

[3] D. Hanna, M. Saavedra-Melo, F. Shan, and F. Capolino, "A versatile polynomial model for reflection by a reflective intelligent surface with varactors," in *IEEE International Symposium on Antennas and Propagation and USNC-URSI Radio Science Meeting (AP-S/URSI)*, 2022, pp. 679–680.